

Synthesis of Tungsten Carbides by Temperature-Programmed Reaction with CH₄–H₂ Mixtures. Influence of the CH₄ and Hydrogen Content in the Carburizing Mixture

J.-M. Giraudon,^{*,1} P. Devassine,^{*} J.-F. Lamonier,[†] L. Delannoy,^{*} L. Leclercq,^{*} and G. Leclercq^{*}

^{*}Laboratoire de Catalyse Homogène et Hétérogène, UPRESA no. 8010, Université des Sciences et Technologies de Lille, 59655 Villeneuve d'Ascq Cédex, France; and [†]Laboratoire de Catalyse et Environnement, M.R.E.I.D., 145 Avenue Maurice Schumann, 59140 Dunkerque Cedex, France

Received November 23, 1999; in revised form June 14, 2000; accepted July 13, 2000; published online September 30, 2000

The influence of the composition of a carburizing CH₄–H₂ gas mixture on the process of reduction–carburization over WO₃ has been studied. Bulk tungsten carbide synthesis has been carried out from WO₃ in different CH₄–H₂ mixtures (CH₄–H₂ = 1/1–3/1; CH₄–N₂ = 1/1; pure CH₄) at atmospheric pressure by temperature-programmed reduction–carburization (TPRC). The composition of the reaction products has been monitored and quantified by gas chromatography analysis (GCA) and the results have been compared to those obtained for a reference sample WC20 (CH₄–H₂ = 1/4). The solids have been characterized by elemental analysis, XRD, XPS, and BET surface area measurements. The overall process is complex. Considering first the reduction, both H₂ and CH₄ act as oxides reducing agents and are converted respectively into H₂O, CO, and to a less extent CO₂. If the reduction steps follow the same sequence observed under pure H₂, WO₃ → W₂₀O₅₈ → WO₂ → W, with the strong difference that W metal is detected only at the surface to be rapidly carburized, the overall reduction process can be accomplished under CH₄–H₂ mixtures at temperatures all the lower than $P_{\text{CH}_4}/P_{\text{H}_2}$ increases. Prereduction of WO₃ into bulk WO₂ allows an easier reduction in practically pure CH₄ (95% (v/v) CH₄–H₂) as reduction with CH₄ increases the rate of the WO₂ → W transformation. Studies of the carburization suggest that CH₄ decomposes on a metallic surface into C (or CH_x) species before bulk WO₂ reduction followed by surface carburization. Then carbon diffuses into the bulk of the solid to give first α-W₂C whose formation occurs rapidly. α-W₂C transformation into WC is slower and seems to be very much influenced by the ratio $P_{\text{CH}_4}/P_{\text{H}_2}$ which controls the rate of carbon deposit at the surface of the solid. The best surface area carbide of 27 m²·g⁻¹ consisting of a core of α-W₂C covered with α-WC has been obtained by using WO₂ as starting material. © 2000 Academic Press

Key Words: tungsten carbide; carbide catalysts; reduction; carburization.

INTRODUCTION

Tungsten carbides are interesting catalytic materials since they are active for several reactions that also occur on group VIII metals (1). But, as previously pointed out by M. Boudart *et al.*, their catalytic application requires the synthesis of materials with high specific surface areas free from pollutants such as polymeric carbon or oxygen (2).

One of the major routes of synthesis for high surface area tungsten carbides has been developed by Boudart and co-workers (2). Their method consists of exposing WO₃ to a reducing–carburizing mixture while heating with a linear temperature program. This method has further been extended to the synthesis of other carbides by Oyama (3,4). The use of an oxide was believed to by-pass the bulk metallic state which is the most prone to sinter (lowest Tammann temperature, which is 1241 K for W compared to 2744 K for WC) (4). By monitoring changes in the exit gas composition by gas chromatography it was shown that the transformation of MoO₃ into an hexagonal Mo₂C with a CH₄–H₂ mixture occurred in two steps. In the first one MoO₃ was reduced into MoO₂ which was clearly identified by XRD measurements. In the second step there was further water formation and methane consumption. The authors were led to the conclusion that simultaneous reduction and carburization occurred (5). Previous works have also been performed by Leclercq *et al.* (6–8) in order to elucidate the complex transformation of tungsten as metal or oxides into the resulting metal carbide by temperature-programmed experiments (TPEs). From these previous results, it is clear that, under the experimental conditions used, carburization occurs only when there is W metal or a suboxide with a very low O content at the surface of the particle. Moreover, carburization of W takes place in two steps, with first the formation of W₂C and then its carburization into WC. Hence, it can be imagined that a way to W carbides with high surface areas would be to form W at the solid surface at

¹To whom correspondence should be addressed. Fax: + 33 3.20.65.61. E-mail: Jean-Marc. Giraudon@univ-lille1.fr.

such a temperature that it can be immediately carburized as soon as it is formed in order to avoid metal sintering. Consequently, for optimizing the W carbide surface areas it is of primary importance to determine what parameters can influence the reduction of WO₃ into W, and the carburization of W.

The purpose of this paper is to improve our understanding of the mechanism of reduction and carburization of WO₃ by each component of the CH₄-H₂ mixture in order to synthesize tungsten carbides at temperatures as low as possible with the aim of developing high surface areas without carbon deposit.

Different syntheses of tungsten carbides have been carried out in CH₄-H₂ mixtures by varying the ratios of the reactants. The bulk of the samples has been characterized by XRD and the related surface by XPS.

EXPERIMENTAL SECTION

The set-up used for the different experiments was previously described (9). To sum up, the syntheses were performed in a plug flow reactor (10 cm long and 2 cm wide) equipped with a thermowell where a thermocouple was settled. Flow rates were regulated by membrane flow regulators (Brooks 8802) and measured with a soap bubble flowmeter. The composition of the effluents at the outlet of the reactor was periodically determined by gas chromatography using a Shimadzu chromatograph GC9A equipped with a thermal conductivity detector (TCD). Analyses were performed every 10 or 20 min with helium as a carrier gas. Products were separated at 110°C in a column (3 m long and 1/8 in. wide) filled with carbosphere molecular sieves. Peak areas were measured with an integrator (Spectra Physics 4270).

Hydrogen (Air Liquide, U quality) was purified by flowing through a Chrompack oxygen clean filter and through 13X molecular sieves. Methane (Air Liquide, N45 quality, 99.995%) was purified by passing through 4A molecular sieves. Nitrogen (Air Liquide, U quality) was passed through copper in short bursts at 350°C in order to remove oxygen impurities and then through 13X molecular sieves. The passivation mixture (2% O₂/N₂, Alphagaz) was used without further purification.

The precursor used to synthesize tungsten carbides in this study was monoclinic WO₃ (Fluka, 99.95%, $S_{\text{BET}} = 3 \text{ m}^2 \cdot \text{g}^{-1}$). Details of the different programmed reduction-carburizations of WO₃ are given in Table 1a.

The bulk structure of the samples was determined by powder X-ray diffraction (XRD) using a diffractometer (Siemens D 5000) ($\text{CuK}\alpha = 0.154178 \text{ nm}$). XRD patterns were ascribed using the JCPDS data base. X-ray photoelectron spectra were obtained with an AEI ES 200B Kratos electron spectrometer equipped with an aluminum anode ($h\nu = 1486.6 \text{ eV}$) or with a VG ESCALAB 220XL. The

binding energies (B.E.s) were referenced either to the C1s peak of polymeric carbon at 285 eV or to the W4f_{5/2} peak of WO₃ at 38.2 eV.

Elemental analyses (EAs) were performed at the "Service Central de Microanalyse" of the CNRS (Vernaison, France). Carbon was transformed into CO₂ in a purified oxygen flow, which was quantified by passing through infrared cells. Oxygen was quantified by the determination of carbon monoxide resulting from the fusion of the sample. W was quantified by plasma emission spectroscopy after fusion of the samples in a NaOH + KNO₃ mixture. Surface areas were measured with a sorptometer (Quantasorb Jr.) using single-point BET surface area determination.

Nomenclature

The samples were labeled WCX (where X is the volumetric percentage of methane in the reactive CH₄-H₂ gas mixture); the suffix N2 is added when dilution of CH₄ is carried out in nitrogen. WCPX referenced to experiments stopped just after the strong peak (P) of methane consumption. The prefix IN was added to characterize intermediates of carburization. WCXY (Y = A, B, C, D) referred to samples submitted to a prereduction of WO₃ into bulk WO₂ or WO₂-W prior carburization in 20% or 95% (v/v) CH₄ in H₂.

RESULTS AND DISCUSSION

1. Reduction-Carburization of WO₃

Figures 1a-1c show three temperature-programmed reduction-carburizations (TPRCs) of WO₃ (Fluka, $3 \text{ m}^2 \cdot \text{g}^{-1}$) performed in CH₄-H₂ mixtures at atmospheric pressure. They are characterized by a set of similar experimental parameters, i.e., an oxide weight of 2 g, a total gas flow rate of $30 \text{ l} \cdot \text{h}^{-1}$, a heating rate of $1^\circ \text{C} \cdot \text{min}^{-1}$, and an isotherm duration of 2 h at the final temperature of 800°C. On the other hand they differ by the methane volumetric percentage which is respectively equal to 50, 75, and 100 in experiments A, B, and C. For all these samples and the others quoted below the synthesis conditions and physical characterizations are reported in Tables 1a and 1b.

In order to study the influence of the CH₄ partial pressure irrespective of that of H₂, a TPRC under conditions similar to those stated above but in a CH₄-N₂ 1/1 mixture (experiment D, compound WC50N2) (Fig. 1d) has been carried out.

For comparison we have added the results of a previous experiment (6) (sample WC1 labeled here WC20, experiment E) carried out in a 20% (v/v) CH₄-H₂ mixture (Fig. 2). It is noteworthy that some main experimental parameters, i.e., the oxide precursor weight (3.5 g), the temperature gradient ($0.83^\circ \text{C} \cdot \text{min}^{-1}$), the gas flow rate ($10 \text{ l} \cdot \text{h}^{-1}$), and the final temperature of treatment (900°C), differ from those given

TABLE 1a
Experimental Conditions of Preparation of Bulk Tungsten Carbides at Atmospheric Pressure

Catalyst	Preparation ^a				Passivation			
	F^b (l.h ⁻¹)	T (°C)	G^c (°C.h ⁻¹)	Duration (h)	Cooling to RT	F (l.h ⁻¹)	% O ₂	Duration (h)
WC20	TC ^d = 10	900	50	10	CH ₄ + H ₂	10	1	15
	TA ^e = 8	800	No	5	H ₂			
WC50	TC = 30	800	60	2	CH ₄ + H ₂	15	0.4	5
	TA = 10	800	No	2	H ₂			
WC75	TC = 30	800	60	2	CH ₄ + H ₂	15	0.4	3.5
	TA = 10	800	No	2	H ₂			
WC100	TC = 30	800	60	2	CH ₄	15	0.4	5
	TA = 10	800	No	2	H ₂			
WC50N2	TC = 30	800	60	2	CH ₄ + H ₂	15	0.4	5
	TA = 10	800	No	2	H ₂			
INWC50	TC = 30	610	60	—	CH ₄ + H ₂	3	2	2
INWC66	TC = 30	550	60	—	CH ₄ + H ₂	3	2	2.5
WCP50	TC = 30	700	60	—	CH ₄ + H ₂	3	2	2
WCP75	TC = 30	680	60	—	CH ₄ + H ₂	3	2	2
WCP85	TC = 30	670	60	—	CH ₄ + H ₂	3	2	2
WC95A	TR ^f = 10	635	60	—	H ₂ + N ₂	3	2	2
	TC = 20	750	60	10	CH ₄ + H ₂			
WC95B	TR = 10	520	120	5	H ₂	3	2	2.
	TC = 20	700	60	10	CH ₄ + H ₂			
WC95C	TR = 10	520	120	4.5	H ₂	3	2	2.
	TC = 20	750	60	27	CH ₄ + H ₂			
WC20D	TR = 10	520	120	4	H ₂	3	2	2.
	TC = 20	750	60	10	CH ₄ + H ₂			

Note. All samples were dried under N₂ to 400–500°C for circa 5 h and cooled to RT before any treatment.

^a WO₃ (2 g) is the precursor for all samples except WC20 (ammonium metatungstate, 3 g).

^b Flow rate (l.h⁻¹).

^c Gradient of temperature (°C.h⁻¹).

^d Treatment of carburization.

^e Treatment of activation in flowing H₂.

^f Treatment of reduction.

TABLE 1b
Bulk and Surface (XPS) Compositions and Specific Surface Areas of Bulk Tungsten Carbides

Catalysts	Temperature of carburization/°C (duration/h)	Composition		BET surface areas/m ² g ⁻¹
		From elemental analysis	From XPS	
WC20 ^a	900(8)	WC _{0.90} O _{0.02}	WC _{3.4} O _{0.23}	10
WC50	800(2)	WC _{0.82} O _{0.50}	WC _{1.3} O _{1.3}	19
WC75	800(2)	WC _{0.67} O _{0.59}	WC _{1.1} O _{1.5}	3
WC100	800(2)	WC _{0.65} O _{0.30}	WC _{1.2} O _{1.6}	9
WC50N2	800(2)	WC _{0.61} O _{0.20}	WC _{1.1} O _{1.7}	6
INWC50	606	WC _{0.1} O _{1.54}	WC _{2.14} O _{0.61}	11
INWC66	560	WC _{0.01} O _{2.31}	WC _{0.29} O _{2.60}	4
WCP50	702	WC _{0.85} O _{0.43}	WC _{2.05} O _{0.41}	14
WCP75	678	WC _{1.16} O _{0.16}	WC _{2.35} O _{1.00}	19
WCP85	670	WC _{1.40} O _{0.056}	WC _{2.76} O _{0.45}	21
WC95A	750(10)	—	—	—
WC95B	700(10)	WC _{1.48} O _{0.1}	—	20
WC95C	750(27)	—	WC _{6.65} O _{0.23}	27
WC20D	750(10)	—	WC _{2.3} O _{0.21}	23

^a From Ref. (6).

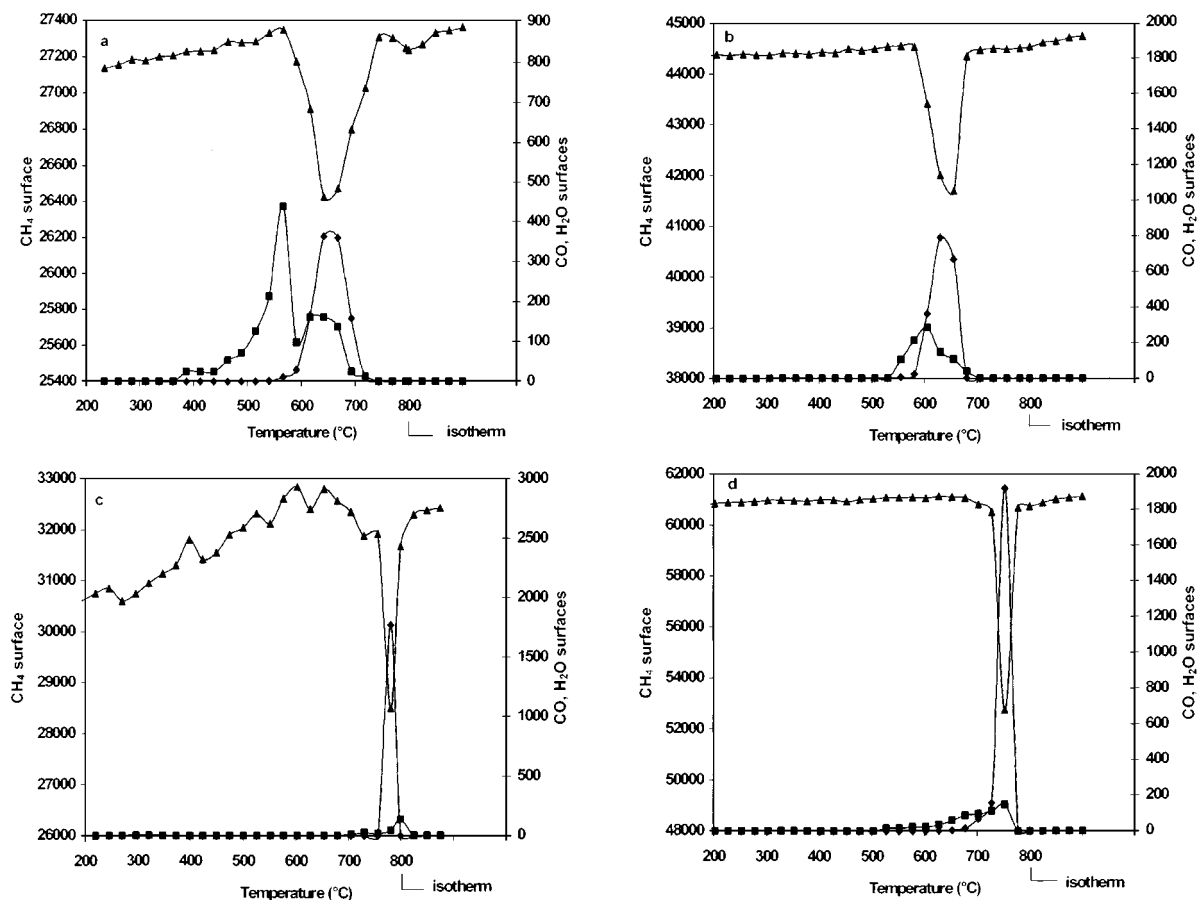


FIG. 1. Variations of the areas of CH₄, H₂O, and CO chromatographic peaks (normalized, taking into account the relative molar response of the TCD) during the reduction-carburizations of WO₃ in the different CH₄-H₂ mixtures (60°C.h⁻¹, 2 g of tungsten trioxide). (a) WC50; (b) WC75; (c) WC50N2; (d) WC100. (▲) CH₄; (■) H₂O; (◆) CO.

above. Table 2 reports the temperatures corresponding to the various events occurring during the experiments, i.e., CH₄ consumption, and CO and H₂O productions. It should be mentioned that the trace of CO₂ which is similar to that of CO but with a significantly lower extent has been omitted for the sake of clarity.

The quantification of the methane consumption and of the oxygen removal has been obtained from gas chromatographic analyses (6).

The amount of oxygen (O/W) removed as CO (CO/W) and H₂O (H₂O/W) during the reduction of the sample together with that of carbon held by the solid (C/W) are shown versus time and temperature in Fig. 3.

(a) Tungsten oxides reduction. Let us first consider the reduction of tungsten oxides. Obviously, not only hydrogen but also methane take part in the reduction of tungsten oxides since not only H₂O but also CO and traces of CO₂ are formed.

Let us first recall the results of a previous temperature-programmed reduction (TPR) of WO₃ (6) at various

H₂ partial pressures. They have clearly shown that the reduction by hydrogen proceeds by three successive steps which seem to correspond respectively to WO₃ → W₂₀O₅₈ (or similar formula) → WO₂ → W (see for example the curve in Fig. 4 reprinted from Ref. (6)). The separation between the different steps is increasingly pronounced as hydrogen pressure decreases. A decrease of P_{H_2} lowers the rates of these three steps but differently since the second step (formation of WO₂) is more influenced than the first one (formation of W₂₀O₅₈) by a change in P_{H_2} , the third step (reduction of WO₂ into W) being itself still more influenced by P_{H_2} . As a consequence, the value of the O/W ratio at the minimum of water production (see Table 3), which probably corresponds to the disappearance of WO₃ (or W₂₀O₅₈), is higher than 1 for a H₂ pressure of 1 atm which shows that the reduction of WO₂ into W starts well before all W₂₀O₅₈ has been reduced into WO₂.

Considering now the reduction of WO₃ in CH₄-H₂ mixtures (Fig. 1, curves a and b and Fig. 2), it can be seen that water production is noticeably influenced by hydrogen pressure since it starts at higher temperatures when P_{H_2}

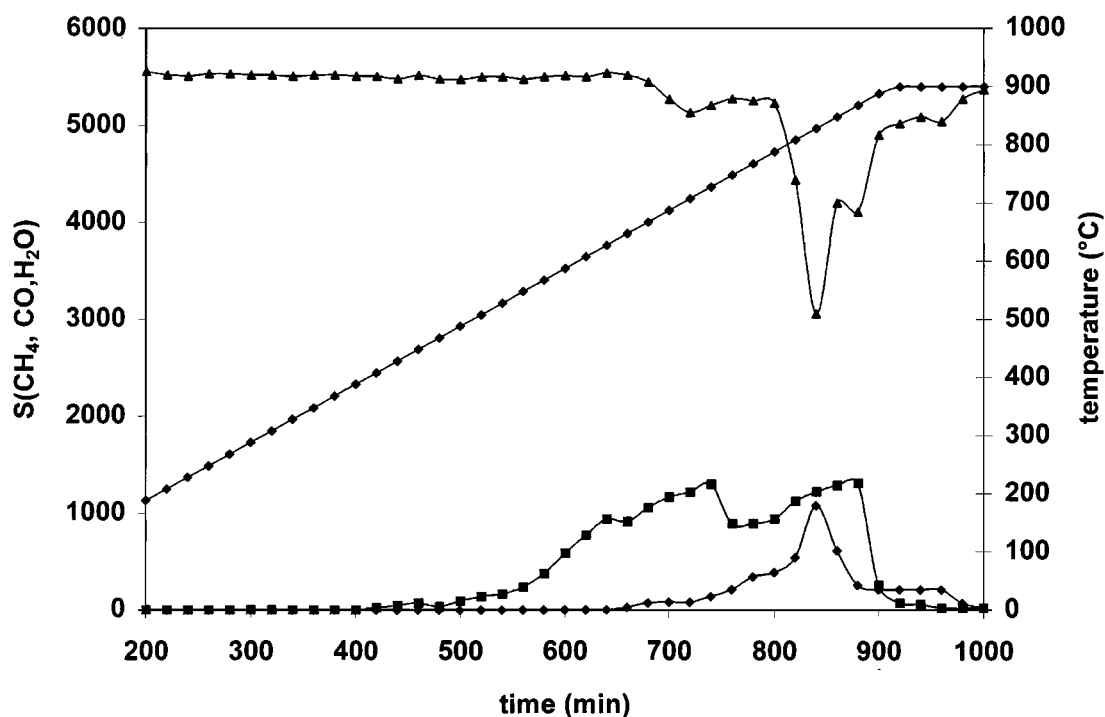


FIG. 2. Variations of the areas of CH_4 , H_2O , and CO chromatographic peaks (normalized, taking into account the relative molar response of the TCD) during the temperature-programmed reduction-carburization of ammonium metatungstate ($50^\circ\text{C}\cdot\text{h}^{-1}$, 3.51 g of ammonium metatungstate) in 20% $\text{CH}_4\text{-H}_2$ (6). (▲) CH_4 ; (■) H_2O ; (◆) CO .

decreases (330, 360, and 530°C for a H_2 pressure of respectively 0.8, 0.5, and 0.25 atm). It also starts before CO formation (whatever the H_2 and the CH_4 pressures, at least in the pressure range studied here) which indicates that, at low temperature, the reduction of WO_3 by H_2 is favored. Water

TABLE 2
Temperatures Relative to the CH_4 Consumption and to the H_2O , CO Productions

	WC20	WC50	WC75	WC100	WC50N2
P_R ($R = \text{CH}_4 + \text{H}_2$)	1 atm	1 atm	1 atm	1 atm	0.5 atm
P_{CH_4}/P_R	0.2	0.5	0.75	1	1
P_{H_2}/P_R	0.8	0.5	0.25	0	0
CH_4 consumption					
θ_i	550	550	580	600	770
θ_{max}	680	640	655	755	780
θ_f	810	730	690	780	790
H_2O production					
θ_i	330	360	530	580	690
θ_{max}	610–720	565–640	610	750	800
θ_f	830	730	700	780	800 (25 min)
CO production					
θ_i	550	540	560	650	770
θ_{max}	700	640	630	750	780
θ_f	810	730	690	780	790

production occurs in, at least, two steps (the initial first step seen in Fig. 4 being mixed with the second step, we will now refer to these two undistinguishable steps as the first one). The shapes of the different profiles of H_2O formation reveal significant changes. Thus the two peaks of water production are well resolved for H_2 pressures of 0.8 or 0.5 atm whereas this is not the case for a hydrogen pressure of 0.25 atm. Furthermore, the relative extent of water production during the second step decreases noticeably as the ratio $P_{\text{H}_2}/P_{\text{CH}_4}$ is lowered, this second step of water production appearing only as a weak shoulder when $P_{\text{H}_2}/P_{\text{CH}_4} = 1/3$ (WC75).

The onset of CO formation occurs during the first peak of water production and seems to be little influenced by $P_{\text{H}_2}/P_{\text{CH}_4}$ in contrast to the amount of CO produced, which increases as $P_{\text{H}_2}/P_{\text{CH}_4}$ decreases (Table 4). This is a result of the competition between H_2 and CH_4 for the reduction of tungsten oxides. The CO production starts for different global degrees of WO_3 reduction (ratios $\text{H}_2\text{O}/\text{W}$), as can be seen in Table 4. It is noticeable that the trace of CO production is very different from that of water, since a single peak is observed even if its shape varies with the gas mixture composition. Moreover, when the step $\text{WO}_3 \rightarrow \text{W}_{20}\text{O}_{58}$ can be distinguished as a shoulder on the first water production peak (Fig. 2 and solids CarbA, B, and C in Ref. (10)), the onset of CO production seems to coincide with the end of that step.

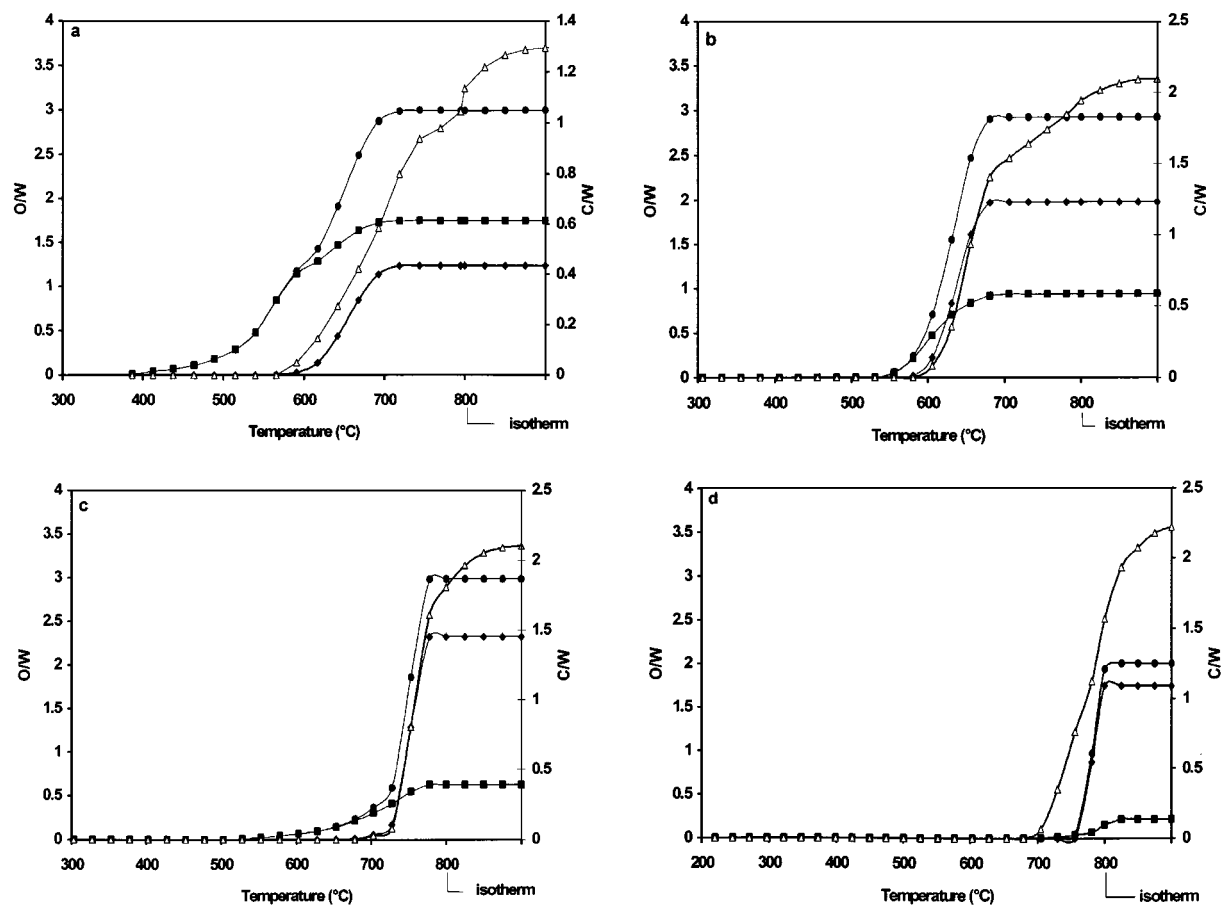


FIG. 3. Evolution of the total oxygen to tungsten: O/W (●) (as water H₂O/W (■) and carbon monoxide CO/W (◆) and carbon (polymeric and carbidic: C/W (△)). Mass balance integrations versus temperature during the temperature-programmed reduction-carburizations of WO₃ in the different CH₄-H₂ mixtures (60°C.h⁻¹, 2 g of tungsten trioxide). (a) WC50; (b) WC75; (c) WC100; (d) WC50N2.

To summarize, two points are remarkable in the W oxides reduction process: the beginning of CO production and the minimum between the two peaks of water formation. In order to get more information we have performed two experiments called INWC66 and INWC50 carried out res-

spectively with H₂-CH₄ mixtures containing 66% and 50% (v/v) of CH₄ and where the reduction process has been stopped respectively when CO started to be detected (560°C) and when the H₂O partial pressure was minimum (610°C). After rapid cooling to room temperature in the reactive mixture flow the solids were passivated as indicated in Table 1a.

First for sample INWC66, at the final temperature of 560°C, the H₂O/W and CO/W ratios respectively of 0.12 and 0.003 lead to a global formula of WO_{2.88}. After passivation its XRD pattern shown in Fig. 5 exhibits mainly the characteristics of W₂₀O₅₈. The decomposition of the complex XPS W4f signal (Fig. 6a) reveals the presence of different oxidic phases (W⁶⁺ ≈ 71%, W^{x+} ≈ 18%, W⁴⁺ ≈ 10%) and of a very small amount of W⁰ (about 1%) at a B.E. of 31.6 eV for the W4f_{7/2} photoelectron peak. Otherwise the C1s signal is very weak and broad (FWHM = 2.7 eV), its position centred at 284.9 eV being characteristic of polymeric carbon.

From the XRD pattern it is clear that CO appearance which indicates the beginning of reduction by CH₄

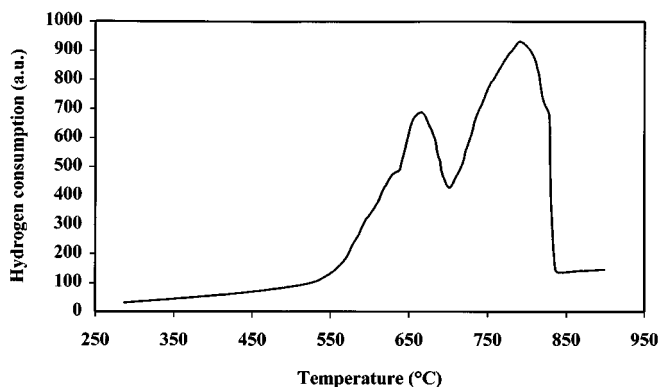


FIG. 4. Temperature-programmed reduction of WO₃ in 30% H₂-Ar (300°C.h⁻¹, 64 mg). TCD signal (in arbitrary units) versus temperature (6).

TABLE 3
O/W (O Consumed per W during Reaction) Ratio as a Function
of P_{H_2} from Ref. (6)

P_{H_2} (atm)	O/W (minimum of H ₂ O production)
0.1	1
0.3	1
1	1.7

corresponds to the WO₃ exhaustion. The bulk of the solid is a suboxide WO_{2.9}, but XPS results show that the surface is more extensively reduced and that CO appearance coincides also with the formation of W⁰ at the sample surface.

For sample INWC50, the ratios H₂O/W and CO/W are respectively 1.2 and 0.2, giving a global formula of WO_{1.6}. Its bulk characterization by XRD (Fig. 5) does not reveal any WO₃ or W₂₀O₅₈ phase and shows WO₂ as the only oxide phase together with small amounts of a reduced phase where W is at zero oxidation degree and which could be W metal or, more probably, α -W₂C. This shows that, as expected from previous results, the subsequent transformation of WO₂ into W has already begun. The XPS W4f signal (Fig. 6b) is very complex and evidences the presence of, at least, four doublets corresponding to W⁶⁺, W^{x+}, W⁴⁺, and W⁰, the W⁰ phase percentage being approximately 11%. The B.E. of 31.9 eV for the photoelectron W4f_{7/2} peak of the reduced component could correspond to a mixture of W metal and of W carbide. These results confirm that the minimum of water production corresponds to the end of W₂₀O₅₈ reduction into WO₂ and, although the reduction of WO₂ into W is slower, it has readily started at that point. Let us note that the CO production is faster during the second peak of H₂O production which corresponds to WO₂ reduction.

All of the above information can be interpreted in terms of competitive reduction of W oxides by H₂ and CH₄. It is clear that the reduction of WO₃ by H₂ is favored at low temperatures compared to that by CH₄ since H₂O formation occurs well before that of CO. This observation is further supported by the fact that reduction of WO₃ occurs

TABLE 4
Characteristics of the Reduction of WO₃

P_{CH_4}	P_{H_2}	Beginning of CO formation	H ₂ O/W
0.2	0.8	550	0.85
0.5	0.5	540	0.5
0.75	0.25	560	0.2
1	0	650	—
0.5	0	770	—

at considerably higher temperatures in the absence of H₂ in the initial gas feed (Figs. 1c and 1d and Table 2). In that case it can be noticed that gas evolution occurs in a short time which probably shows that the slow step of the process is the reduction of WO₃, the further suboxides reduction being fast. Considering the reduction of W oxides by CH₄, evidenced by CO formation, its participation increases with the ratio P_{CH_4}/P_{H_2} since the ratio H₂O/CO of the number of moles of H₂O and CO produced during the reaction is 0.3, 0.5, 1.4, and 3.8 for ratios P_{CH_4}/P_{H_2} of 4, 1, 0.33, and 0.

Then a question arises: why does CO appear later than H₂O? There could be three possibilities:

(i) CH₄ and H₂ can reduce tungsten oxides but the energies of activation of the rate constants of reduction by CH₄ are higher than those related to reduction by hydrogen.

(ii) CH₄ is only slightly active for WO₃ reduction (see Figs. 1c and 1d), but it is better for the reduction of a W suboxide. This suboxide would probably not be W₂₀O₅₈ since CO is not seen during the first step of reduction (WO₃ → W₂₀O₅₈) but more likely WO₂, since CO production increases rapidly during the second H₂O peak.

(iii) CO appearance could be related to the formation of a metal phase at the solid surface where CH₄ could be activated by chemisorption (either as CH_x or as C) to further react for the reduction of the remaining W suboxides. Here, let us recall a previous study (10), which shows that CO production during a TPRC of WO₃ with a CH₄/D₂ mixture begins simultaneously at the onset of CH₄-D₂ exchange. Since this exchange reaction is likely to occur only on metal, this is probably another indication, in addition to the XPS study on the INWC66 sample, of the high surface reduction when CO formation starts. However, if it is clear that CO appearance is an indication of the presence of a metal phase at the solid surface, at that stage it is not possible to know whether CO and metal are simultaneously formed during WO₂ reduction by gaseous CH₄ or if the presence of W metal at the surface due to the WO₂ reduction is a condition for CH₄ adsorption before it can reduce WO₂.

In order to check the first hypothesis (i) we have performed a TPRC of WO₂ (Fig. 7). It was prepared by TPR of WO₃ in a H₂-N₂ (1/1) mixture in order to have a better separation between the two H₂O peaks, from room temperature until the minimum of water production was reached (635°C). The corresponding O/W ratio was 1.1 and the effectiveness of the complete transformation of WO₃ into WO₂ was ascertained by XRD. After cooling to room temperature the sample was heated to 750°C (60°C.h⁻¹) in a CH₄-H₂ (95/5) gas mixture (20 l.h⁻¹) and kept in an isotherm for 10 h (sample WC95A). Considering the subsequent oxygen removal, CO was the only oxygen-containing product in the gas phase (CO/W = 1.8). It began to be detected at 470°C, which is much lower than for samples

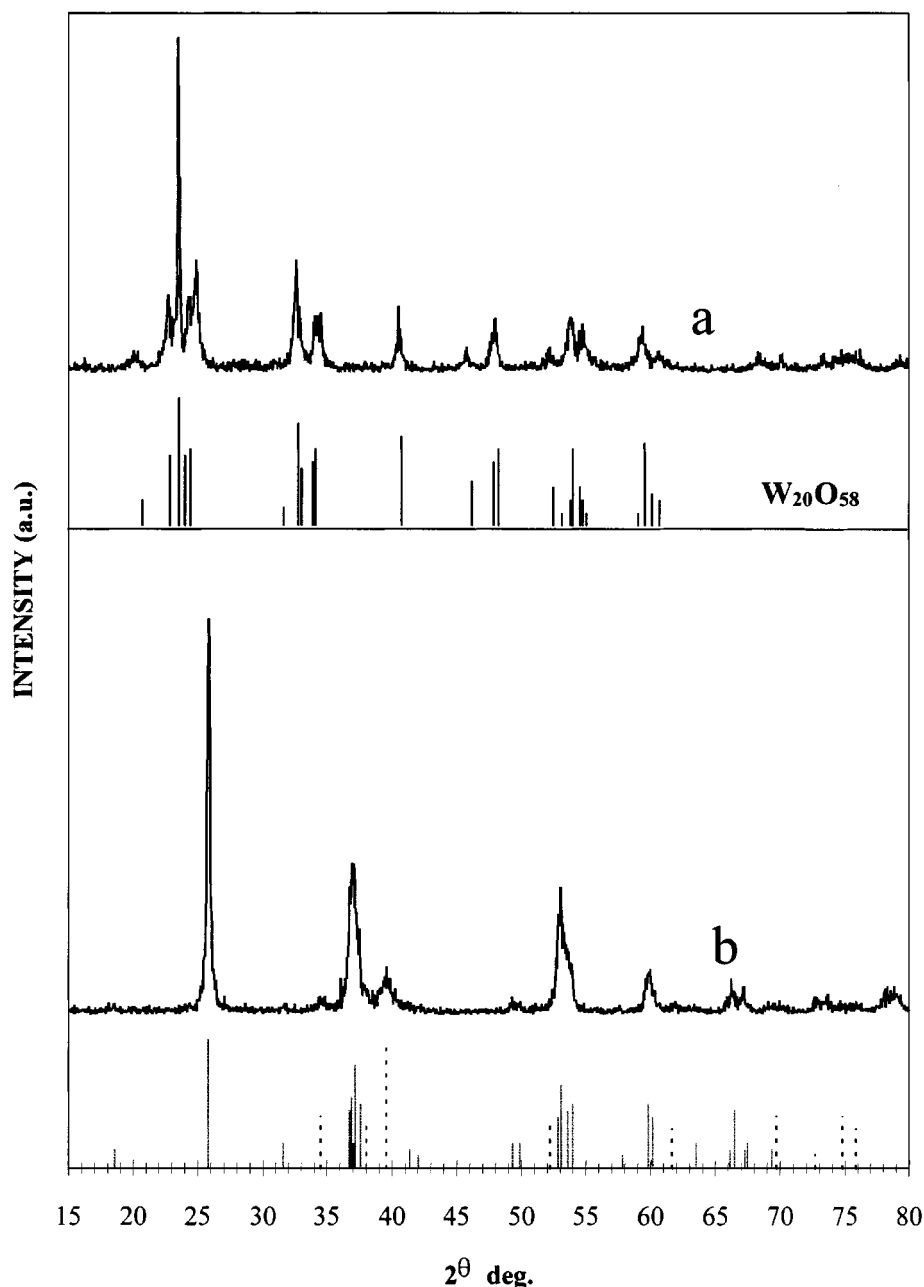


FIG. 5. (a) X-ray diffraction pattern of the INWC66 sample; beneath are the lines of W₂₀O₅₈. (b) X-ray diffraction pattern of INWC50 samples; beneath are the lines of WO₂ (—) and W₂C (---).

WC20, -50, and -75 (540°C to 560°C). CO production was maximum around 630°C before disappearing at 670°C. Consequently, the overall reduction process occurred at a lower temperature than in experiments WC20, -50 and -75, which implies that explanation (i) may be ruled out. On the other hand, it is clear that CH₄ is more effective in the reduction of WO₂ than in that of WO₃ (compare with experiment C or D). However, this experiment does not

allow us to choose between the second and the third hypotheses.

Going further, if it is assumed, as suggested above, that H₂ is the only species which reduces WO₃ into WO₂ via W₂₀O₅₈ formation, at least when its partial pressure is not too low, it is possible to calculate the ratio [(H₂O/W) - 1/(CO/W)] of the number of moles of H₂O and CO produced during the reduction of WO₂ into W (Table 5).

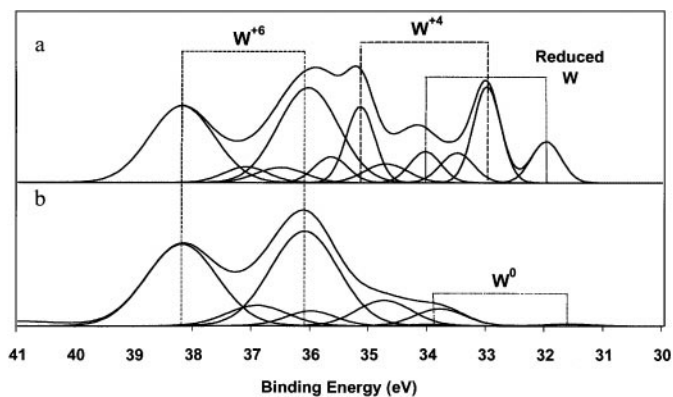
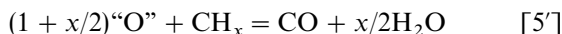
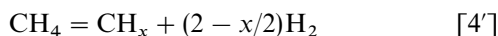
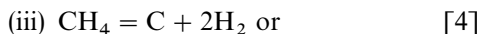
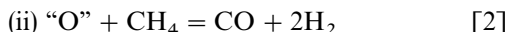
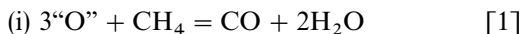


FIG. 6. (a) XPS W4f signals of the INWC50 sample. (b) XPS W4f signals of the INWC66 sample.

Considering, as an example, the value obtained for equal pressures of H₂ and CH₄ of 0.6, it is clear that CH₄ is a better reducing agent for WO₂ reduction than H₂.

Concerning the reduction by CH₄, several possibilities can be considered:



where, "O" is an oxygen moiety in tungsten oxides. Obviously, the first hypothesis does not agree since the ratio H₂O/CO for WO₃ reduction by CH₄-H₂ mixtures should be higher than or equal to 2, which is obviously not the case for WC50, -75, -100, and -50N2 (Table 5). Hypotheses (ii) and (iii) are both reasonable.

(b) *Carburization.* We will now examine the results of the carbon formation from CH₄ (either for carburization or as polymeric carbon). All of the CH₄ consumption profiles (Fig. 1) exhibit a strong peak (except WC20 which shows a supplementary shoulder) which evidences a residual consumption, the peak being sharper as $P_{\text{CH}_4}/P_{\text{H}_2}$ is higher. It is remarkable that the strong production of carbon (either

carbide or polymeric) is observed in the same temperature range as that of CO with a lower ending temperature as CH₄ pressure increases (810, 730, and 690°C for CH₄ pressures of respectively 0.2, 0.5, and 0.75 atm). Finally the retention of carbon by the solid (C/W) increases as $P_{\text{H}_2}/P_{\text{CH}_4}$ drops (Table 6).

Consequently, it seems that carburization begins to proceed as soon as some W metal is formed if CO is really an indication of W formation. This observation is very much in agreement with previous conclusions reported in Ref. (6) where we mentioned that carburization takes place only when W metal is present at the surface of the solid. Let us note that the simultaneous reduction of WO₂ into W by CH₄ and CH₄ conversion into carbide or amorphous carbon can be another argument for CH₄ decomposition before bulk WO₂ reduction, C (or CH_x) species deposited at the surface being either oxidized by O species of the tungsten oxides, incorporated into W metal for carburization, or left at the solid surface as an amorphous deposit.

In order to understand what happens at the end of the strong methane consumption and to characterize the solids at that stage, three TPRCs (samples WCPX, X = 50, 75, 85) have been carried out and stopped at the end of the strong

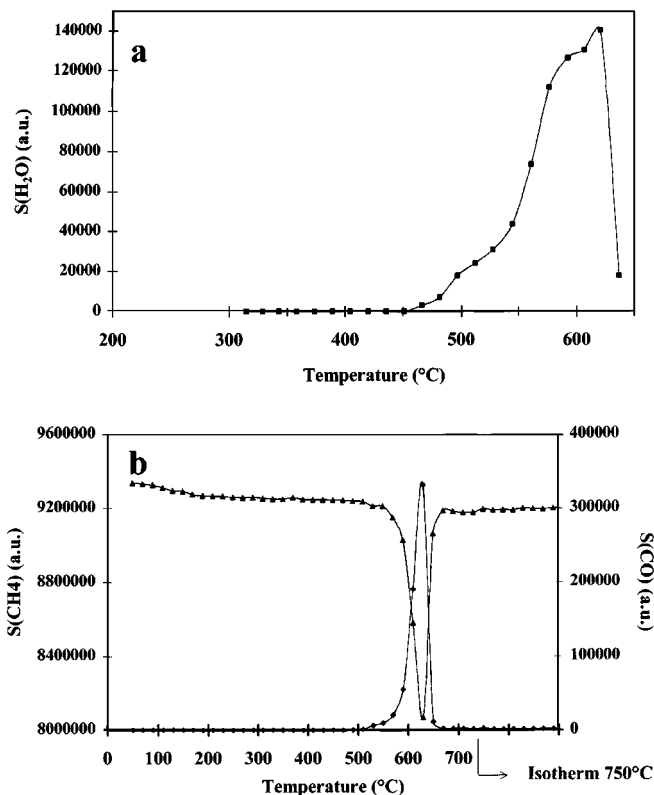


FIG. 7. (a) Temperature-programmed reduction of WO₃ ($m = 2.046$ g, $60^\circ\text{C}\cdot\text{h}^{-1}$) to WO₂ in a 1/1 H₂-N₂ mixture (total flow rate, $10\text{ l}\cdot\text{h}^{-1}$). (b) Subsequent carburization profile of WC95A in a 95/5 CH₄-H₂ mixture ($20\text{ l}\cdot\text{h}^{-1}$, $60^\circ\text{C}\cdot\text{h}^{-1}$, $\theta_{\text{max}} = 750^\circ\text{C}$ for 10 h).

TABLE 5
Mass Balance Calculations Concerning the Reduction of WO₃

	WC20	WC50	WC75	WC100	WC50N2
P_{CH_4} (atm)	0.2	0.5	0.75	1	0.5
P_{H_2} (atm)	0.8	0.5	0.25	0	0
$[(\text{H}_2\text{O}/\text{W} - 1)/(\text{CO}/\text{W})]$	2.1	0.6	≈ 0	—	—
H ₂ O/CO	3.8	1.4	0.47	0.27	0.12

CH₄ consumption which corresponds to an ending temperature of 702, 678, and 670°C for respectively WCP50, -75, and -85. The samples were then rapidly cooled to room temperature before being passivated. Mass balance calculations from elemental and chromatographic analyses give C/W ratios of 0.85 (0.92), 1.16 (1.19), 1.40 (—), respectively, for WCP50, -75 and -85. The resulting XRD are in Fig. 8. That of WCP50 clearly exhibits only the hexagonal closed-packed α -W₂C phase whereas those of WCP75 and WCP85 are poorly resolved, showing particularly broad lines in the 30–45° 2 θ windows. The very broad lines cannot be explained only by the presence of small W₂C particles and probably attest that the solid is not well organized. One notices besides a very small contribution of the hexagonal α -WC phase, this one being more extensive as $P_{\text{CH}_4}/P_{\text{H}_2}$ is higher.

From these results it is clear that carburization into WC is far from being complete at the end of the CH₄ consumption peak. When all oxygen has been practically removed from the initial solid, only α -W₂C is formed for a ratio $P_{\text{CH}_4}/P_{\text{H}_2}$ of 1 whereas the successive transformation of W₂C into WC has already begun for the higher ratios.

In order to remove the excess polymeric carbon which is always deposited at the sample surface during the carburization process (11) samples WC50, -75, -100, and -50N2 have been submitted *in situ* to a cleaning treatment in pure flowing H₂ (10 l.h⁻¹) just after carburization at 800°C for 2 hours. The CH₄ trace is rather similar to that given in

TABLE 6
Characteristics of the Different Carbides: Mass Balance Ratios of Carbon Held by the Solid at the End of the Strong Peak of Methane Production* and at the End of the Carburization**

Samples	(C/W) _p *	(C/W) _F **
WC50	0.94	1.3
WCP50	0.92	—
WC75	1.40	2.1
WCP75	1.19	—
WCP85	1.4	—
WC100	1.8	2.1
WC50N2	1.6	2.2

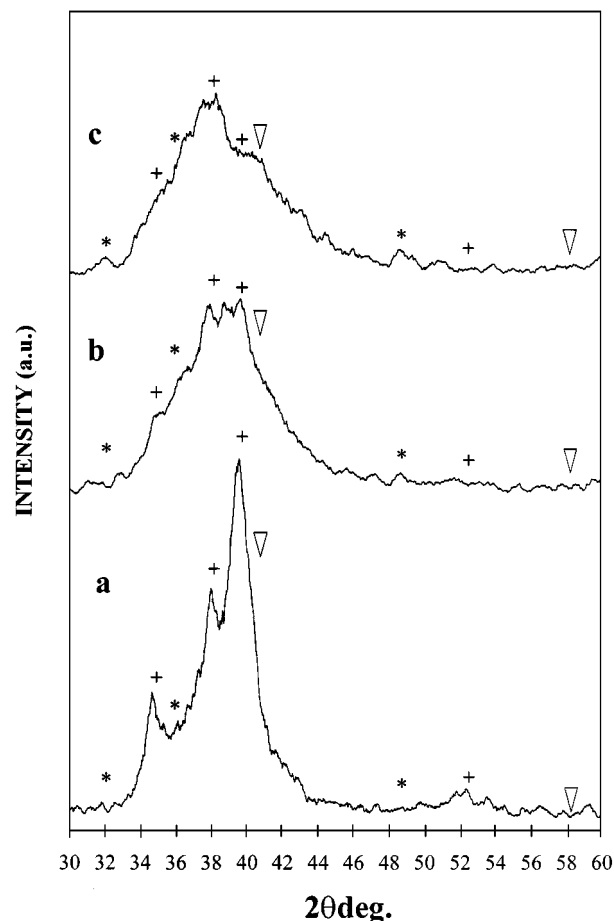
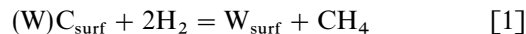


FIG. 8. XRD of the passivated WCP50 (a), WCP75 (b), and WCP85 (c) samples prepared from temperature-programmed reduction-carburizations of WO₃ respectively in CH₄ 50–75–85 (v/v) in H₂ and stopped at 700°C (WCP50), 680°C (WCP75), and 670°C (WCP85). Above are represented the characteristic patterns of WC (*), α -W₂C (+), and W (▽) extracted from the JCPDS data files.

Fig. 1 of Ref. 11, which showed a slow CH₄ decrease until a weak and stable value of CH₄ was reached. It has been shown that the strong CH₄ production at the beginning of the treatment probably arises from the excess carbon elimination, while the residual CH₄ pressure at the stationary state has been ascribed to a slow process of decarburization (12, 13). The elimination of carbidic carbon can result from the two successive steps:



At 800°C, the experimental P_{CH_4} ($6-7 \times 10^{-4}$ atm) is very close to that of the equilibrium of reaction [1] (about 8.7×10^{-4} atm). Consequently, steps [1] and [2] respectively of partial surface decarburization and of carbidic carbon diffusion from the bulk to the surface are probably fast.

After this cleaning procedure, the solids were cooled in flowing H_2 to room temperature and submitted to a simple nitrogen sweep before being passivated in an O_2-N_2 (0.4/99.6) mixture. Finally the samples WC50, -75, -100, and 50N2 were characterized by EA, XRD, and XPS. The elemental analysis results given in Table 1b show that the synthesis process for these samples leads to incomplete carburization (C/W atomic ratio less than 1). The XRD patterns of the four samples are displayed in Fig. 9. Sample WC50 corresponds to a major α -WC phase with a minor phase which could be α - W_2C phases or a mixture of α - W_2C with W metal. The others patterns are qualitatively similar, but with a higher proportion of α - W_2C as the CH_4 content in the feed is higher. This is probably due to a too short duration of the carburization isotherm at $800^\circ C$. These results may seem to be in contradiction with the previous ones on the samples WCPX. We will come back later on these points.

Surface characterizations performed by XPS experiments led to corresponding photoelectron W4f, C1s, and O1s peaks having a general aspect similar to those observed for

the WC20 sample (6). By way of example a decomposition of the C1s, W4f, and O1s photoelectron peaks for the WC50 sample is exhibited in Fig. 10. The C1s peak shows a well-defined carbidic component at low B.E. (283.2 ± 0.2 eV); the other components at higher B.E. are associated with carbon linked with oxygen as previously noted (6). The W4f peak consists of, in any case, two main doublets characteristic respectively of the reduced and oxidic forms (W^{6+}). The B.E. of the W4f_{7/2} photoelectron peak from the more reduced doublet arises at 32.2 ± 0.2 eV for all samples, confirming that tungsten is in its carbidic form (6). Besides, the O1s signal is typically asymmetric and has a B.E. of 531 eV characteristic of oxygen bound to tungsten in transition (+6) oxides.

The surface areas of the solids are listed in Table 1b. It can be seen that the surface area of WC50 is the highest of the four samples ($19 \text{ m}^2 \cdot \text{g}^{-1}$) and higher than those of most WCs obtained in a H_2-CH_4 1/4 gas mixture (6). In contrast, WC75, -100, and -50N2 have low surface areas, obviously smaller than those obtained without hydrogen cleaning treatment.

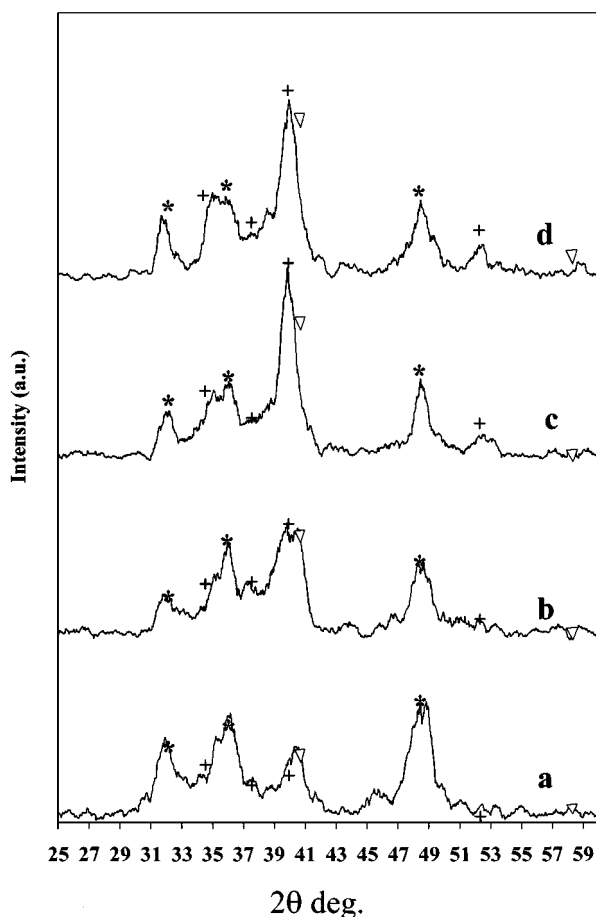


FIG. 9. X-ray diffraction patterns of the different carbides. (a) WC50; (b) WC75; (c) WC100; (d) WC50N2. WC (*), α - W_2C (+), W (∇).

2. Reduction-Carburization of WO_2

The final objective of these studies is to try to select optimum experimental conditions for the synthesis of W carbides (mainly α -WC) with surface areas as large as possible. In order to improve the surface areas of the carbides it seems desirable to carburize at the lowest temperature possible. Thus W metal should be carburized as soon as it is formed in order to decrease the temperature of the overall process and to avoid sintering at high temperature. Since, in the first part of this study, it has been seen that CH_4 is likely to be more efficient for the $WO_2 \rightarrow W$ transformation than H_2 and that the carburization proceeds faster as P_{CH_4}/P_{H_2} increases, one might envision separating the overall reduction-carburization process into two steps. The first one will be the formation of a well-defined WO_2 species that will further be reduced and carburized in a CH_4 -enriched methane/hydrogen mixture.

Our purpose being to synthesize α -WC, taking into account the previous results from experiments WCPX, seeming to indicate that a higher P_{CH_4} in the early stages of carburization led to the formation of higher WC percentages, we first performed the reduction-carburization of WO_2 in a CH_4-H_2 mixture (95/5). The procedure was the following:

(i) WO_3 was first reduced in pure flowing hydrogen from room temperature to $520^\circ C$ until water production significantly decreased and was left for about 2 h at that temperature. The ratio O/W corresponding to WO_3 reduction by H_2 was about 1.4–1.5. XRD results show the presence of WO_2 and of some W metal (Fig. 11).

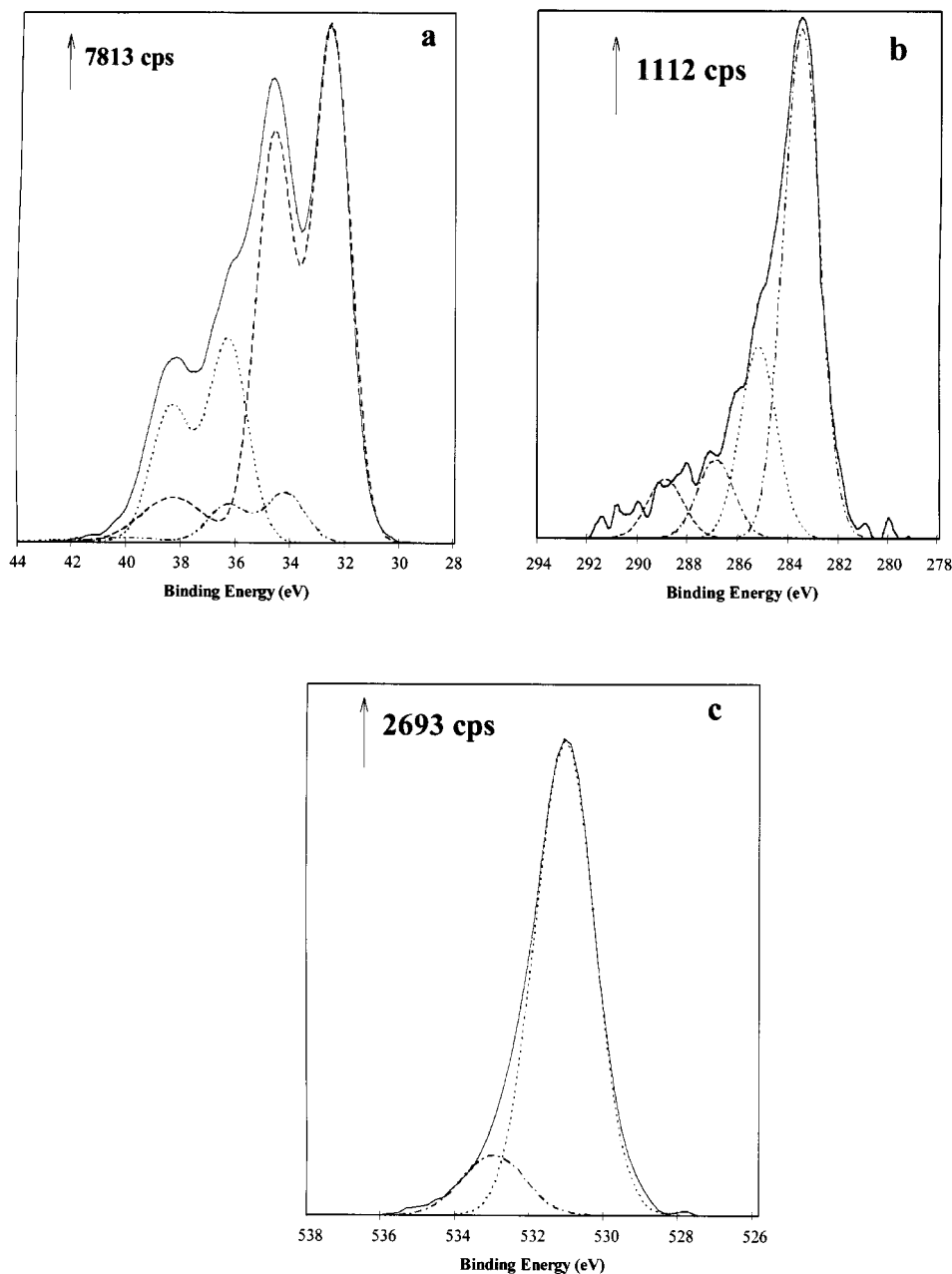


FIG. 10. Decomposition of the W4f (a), C1s (b), and O1s (c) XPS peaks of WC50.

(ii) After the reactor was cooled to room temperature, H₂ was replaced by the CH₄-H₂ 95/5 mixture (20 l.h⁻¹). The solid was then heated (60°C.h⁻¹) to a chosen temperature (700°C, WC95B or 750°C, WC95C, and left for several hours in an isotherm before being cooled to room temperature and passivated.

(a) *Reduction of WO₂*. The trace of CO for experiment WC95B is shown in Fig. 12 and compared to that of sample WC95A. It is shown that, while the temperature range for

CO formation is the same for both experiments (470–670°C), CO partial pressure is, in the early stages of the reduction, significantly lower for experiment WC95A than for WC95B. Considering that the extent of the initial oxide reduction was lower for the first experiment (O/W = 1.1) as calculated from the amount of water evolved during the production of WO₃ than for the second one (1.4) as also evidenced by XRD (hence the amount of W metal at the sample surface was probably lower), this can be explained by the necessity for CH₄ to be activated by adsorption on

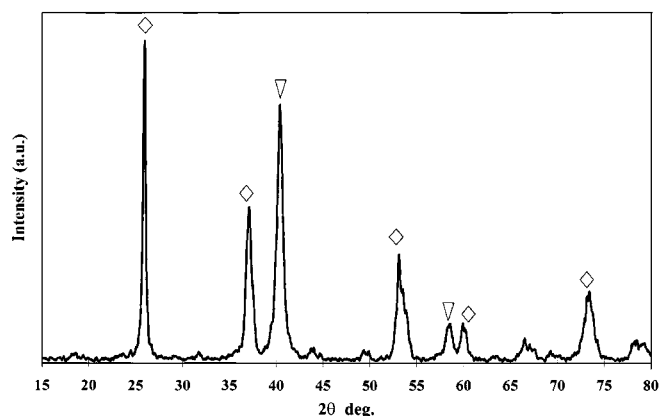


FIG. 11. XRD of WO_3 ($m = 2$ g) reduced in flowing H_2 (10 l.h^{-1}) from room temperature to 520°C (120°C.h^{-1} , 4 h in isotherm). WO_2 (\diamond), W (∇).

W metal before being active in W oxides reduction. Consequently, this would be in favor of the third explanation (iii) proposed above for the influence of the ratio $P_{\text{CH}_4}/P_{\text{H}_2}$ on H_2O and CO formation during oxide reduction. However, we think that this argument should not be considered as a definite proof.

(b) *Carburization.* A first attempt of carburization following the above procedure was performed with a maximum temperature of 700°C (WC95B), which was maintained for 10 h. XRD characterization (Fig. 13) shows that carburization was far from being complete since $\alpha\text{-W}_2\text{C}$ was the major phase formed during this experiment with only along a small percentage of $\alpha\text{-WC}$. The global formula obtained from EA which is $\text{WC}_{1.48}\text{O}_{0.1}$ attests to a strong carbon deposit of polymeric carbon. Another preparation starting from a very similar $\text{WO}_2 + \text{W}$ mixture after reaction at 750°C for 27 h (WC95C) led to a more extensive carburization (Fig. 13) but it is still incomplete since $\alpha\text{-W}_2\text{C}$ is again detected which can seem rather surprising consider-

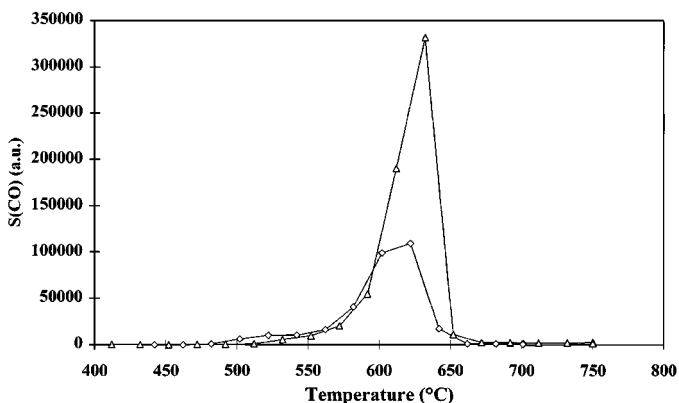


FIG. 12. CO traces of WC95A (\triangle) and WC95B (\diamond) versus temperature obtained during the reduction-carburizations of these samples in $\text{CH}_4\text{-H}_2$ (95/5) gas mixtures (60°C.h^{-1}).

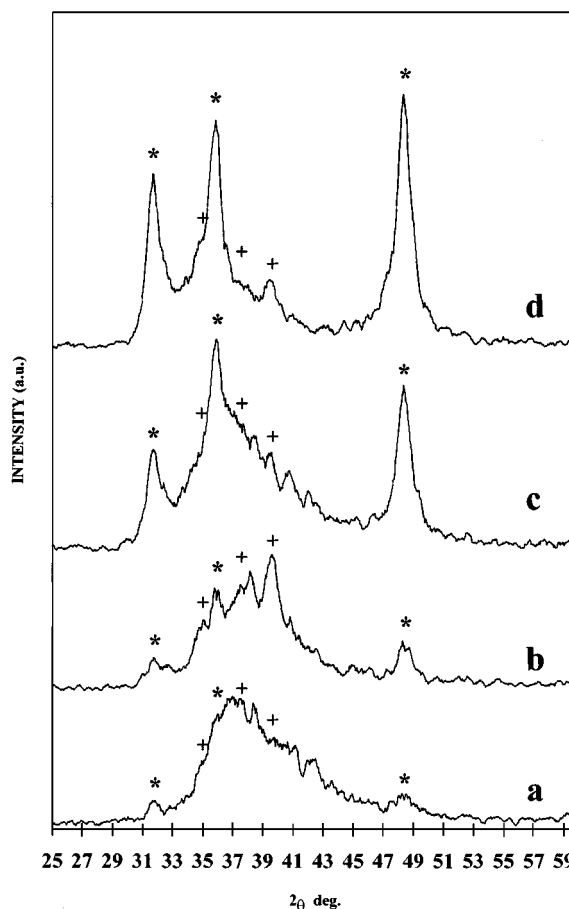
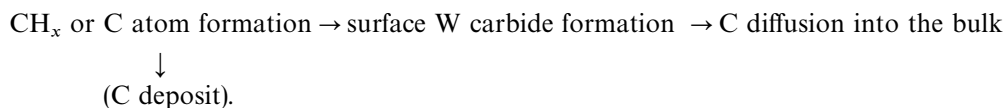


FIG. 13. XRD patterns of the passivated samples WC95A (a), WC95B (b), WC95C (c), and WC20D (d) prepared by temperature-programmed reduction-carburizations of prerduced WO_3 (2 g) (see Table 1a) in $\text{CH}_4\text{-H}_2$ (95/5) gas mixtures, except for WC20D in (20/80) (60°C.h^{-1} , 30 l.h^{-1}) respectively to $750\text{-}700\text{-}750^\circ\text{C}$ for 10-10-27-10 h (WC95A, WC95B, WC95C, WC20D).

ing that carburization in a mixture $\text{CH}_4\text{-H}_2$ 1/4 led to the complete carburization into WC at 750°C , to a high percentage of WC at 700°C (6), and to the apparently faster carburization in $\text{CH}_4\text{-H}_2$ mixtures when the ratio $P_{\text{CH}_4}/P_{\text{H}_2}$ increases as seen earlier.

However, these observations correlated with those obtained from WCX and WCPX syntheses can be rationalized in the following way:

Methane starts to be adsorbed on the reduced surface (either W or surface W carbide) where it dissociates into H_{ads} and CH_x fragments or C atoms at the solid surface. Such an adsorption and decomposition is favored by higher P_{CH_4} (adsorption) and lower P_{H_2} (decomposition). As soon as CH_x or C is formed it can be incorporated into the solid as surface carbide and diffuse into the bulk, leading to bulk carbides, or polymerize to form the carbon deposit. The competition of these two processes is a function of temperature. Of course, when the solid surface gets covered by the



SCHEME 1

polymerization carbon deposit, CH₄ adsorption and consequently CH_x or C atom formation is decreased as is the feeding of the solid bulk with C atoms; hence, WC formation would stop even under conditions where usually it should be complete in the absence of such surface blocking by C deposit. The layer of polymerized carbon is assumed to be inefficient in the carburization processes. The reaction scheme is shown in Scheme 1.

These four steps are influenced differently by temperature and $P_{\text{CH}_4}/P_{\text{H}_2}$. At a given temperature the first step (CH_x or C formation) is favored by high $P_{\text{CH}_4}/P_{\text{H}_2}$ ratios as seen above which will increase the surface coverage with individual C adsorbed species (with only one carbon). Consequently, the rates of the two others steps of surface W carbide formation and of C polymerization will also increase as $P_{\text{CH}_4}/P_{\text{H}_2}$ increases. But while the W carbide formation is probably first order in the CH_x (or C atom) surface concentration, the carbon polymerization will increase faster as the CH_x surface concentration increases, and also the blocking of the solid surface, resulting in a decrease of the rates of CH₄ adsorption and decomposition and of surface and bulk carbides formation. When the solid surface is completely covered with polymerized carbon the carburization process stops because the solid surface can no longer be fed by monoatomic C species. Hence, this mechanism explains well why carburization starts at lower temperatures when $P_{\text{CH}_4}/P_{\text{H}_2}$ is increased since the rates of the processes increase but it also explains why carburization can stop before being complete.

A consequence of the above observations is that a mixture H₂-CH₄ with lower CH₄ concentrations could be preferable to obtain more easily pure α -WC; since it is well known that H₂ is an inhibitor for alkanes adsorption (14), a higher H₂ pressure will lower CH₄ adsorption and its further decomposition. Consequently, the rate of carbon deposition could be adapted to that of C diffusion into the bulk of the solid by adjusting H₂ and CH₄ pressures to an optimum value. A final experiment has been performed on a prereduced sample in a CH₄-H₂ 1/4 mixture at 750°C for 10 h (WC20D, Table 1a). The solid obtained was mainly α -WC (XRD, Fig. 13) with only a very small amount of α -W₂C. Its surface area was 23 m².g⁻¹. This result seems to confirm the above reasoning.

These attempts at improving the W carbides surface areas by using WO₃ prereduced into a mixture WO₂-W were successful since the solids obtained had higher surface areas than those obtained in our laboratory by reduction-carburization of WO₃ by CH₄-H₂ mixtures. The optimization of

the preparation conditions will have to be done by playing on the CH₄/H₂ mixture composition, the maximum temperature, the duration of carburization, and the space velocity of the carburizing mixture. Until now, the best surface area obtained was 27 m².g⁻¹ for sample WC95C, which is a core of W₂C surrounded by WC at its surface.

CONCLUSION

The influence of the composition of a carburizing CH₄-H₂ gas mixture on the process of reduction-carburization over tungsten oxides has been studied. This process has been shown to be very sensitive to the ratio $P_{\text{CH}_4}/P_{\text{H}_2}$ of the reactive gas. The solids have been characterized by XRD and XPS at various extents of reaction. The overall process is complex and starts at low temperature with the reduction of WO₃ and W₂₀O₅₈ by hydrogen. Then, as soon as WO₂ is formed at the surface of the solid, reduction by CH₄ occurs as evidenced by CO formation, this reduction being favored compared to that by H₂. This step is likely to occur via adsorption and decomposition of CH₄ on W metal formed at the surface by WO₂ reduction and reaction of C atoms or of CH_x fragments with oxygen atoms of the solid, although this has not yet been definitively proved. The carburization process starts with monoatomic carbon deposition (as C atoms or as CH_x adsorbed species) at the W surface and surface carburization. Carbon species then diffuse into the bulk of the solid to form, first, α -W₂C whose formation occurs rapidly. WC formation by carbon diffusion into W₂C is slower and can be incomplete when the ratio $P_{\text{CH}_4}/P_{\text{H}_2}$ is higher. This phenomenon is probably related to the extent of polymeric carbon formation at the solid surface. The reduction-carburization of WO₃ has been compared to that of WO₂ prepared by previous reduction of WO₃ by hydrogen. The overall process occurs at lower temperatures when using WO₂ and higher surface areas are obtained for the resulting W carbides; the best surface area obtained was 27 m².g⁻¹ for a solid composed of a core of W₂C covered with WC. This surface is about twice that of the WC usually obtained by WO₃ carburization. All of these observations will be a guideline to control and optimize the synthesis of the carbides.

ACKNOWLEDGMENTS

We thank Mr. L. Gengembre for performing the XPS analysis, Ms. Burylo for performing the X-ray diffraction studies, and Dr. A. Löfberg for helpful discussions.

REFERENCES

1. S. T. Oyama, *Catal. Today* **15**, 179 (1992).
2. E. Iglesia, F. H. Ribeiro, M. Boudart, and J. E. Baumgartner, *Catal. Today* **15**, 445 (1992).
3. S. T. Oyama, Ph.D. Dissertation, Stanford University, 1981.
4. S. T. Oyama, J. C. Slatter, J. E. Metcalfe, and J. M. Lambert, Jr., *Ind. Eng. Chem. Res.* **27**, 1639 (1988).
5. J. S. Lee, S. T. Oyama, and M. Boudart, *J. Catal.* **106**, 125 (1987).
6. G. Leclercq, M. Kamal, J.-M. Giraudon, P. Devassine, L. Feigenbaum, L. Leclercq, A. Frennet, J. M. Bastin, A. Löfberg, S. Decker, and M. Dufour, *J. Catal.* **158**, 142 (1996).
7. G. Leclercq, M. Dufour, A. El Gharbi, J.-M. Giraudon, M. Kamal, J. F. Lamonier, and L. Leclercq, *Bull. Soc. Chim. Belg.* **105**, 2 (1996).
8. A. Frennet, G. Leclercq, L. Leclercq, G. Maire, R. Ducros, M. Jardinier-Offergeld, F. Bouillon, J. M. Bastin, A. Löfberg, P. Blehen, M. Dufour, M. Kamal, L. Feigenbaum, J.-M. Giraudon, V. Keller, P. Wehrer, M. Cheval, F. Garin, P. Kons, P. Delcombe, and L. Binst, in "Proceedings of the 10th Congress on Catalysis" (L. Guzzi, F. Soymost, and P. Tetenyi, Eds.), pp. 927-937. Akademia Kiado, Budapest, 1993.
9. G. Leclercq, L. Leclercq, and R. Maurel, *J. Catal.* **5**, 87 (1977).
10. A. Löfberg, A. Frennet, G. Leclercq, L. Leclercq, and J.-M. Giraudon, *J. Catal.* **189**, 170 (2000).
11. G. Leclercq, M. Kamal, J. F. Lamonier, L. Feigenbaum, P. Malfroy, and L. Leclercq, *Appl. Catal.* **169**, 121 (1995).
12. F. H. Ribeiro, R. A. Dalla Betta, M. Boudart, J. E. Baumgartner, and E. Iglesia, *J. Catal.* **130**, 86 (1991).
13. F. H. Ribeiro, R. A. Dalla Betta, G. J. Guskey, and M. Boudart, *Chem. Mater.* **3**, 805 (1991).
14. A. Frennet, in "Hydrogen Effects in Catalysis" (Z. Paal and P. G. Menon, Eds.), pp. 399-423. Dekker, New York, 1988.